

Osteosarcoma growth on trabecular bone mimicking structures manufactured via laser direct write

Atra Malayeri¹, Colin Sherborne², Thomas Paterson², Shweta Mittar², Ilida Ortega Asencio¹, Paul V. Hatton^{1*} and Frederik Claeyssens^{2**}

¹ Bioengineering and Health Technologies Group, The School of Clinical Dentistry, University of Sheffield, Sheffield S10 2TA, United Kingdom

² Biomaterials and Tissue Engineering Group, Department of Materials Science and Engineering, Kroto Research Institute, University of Sheffield, Sheffield S3 7HQ, United Kingdom

Abstract: This paper describes the direct laser write of a photocurable acrylate-based PolyHIPE (High Internal Phase Emulsion) to produce scaffolds with both macro- and microporosity, and the use of these scaffolds in osteosarcoma-based 3D cell culture. The macroporosity was introduced via the application of stereolithography to produce a classical “woodpile” structure with struts having an approximate diameter of 200 μm and pores were typically around 500 μm in diameter. The PolyHIPE retained its microporosity after stereolithographic manufacture, with a range of pore sizes typically between 10 and 60 μm (with most pores between 20 and 30 μm). The resulting scaffolds were suitable substrates for further modification using acrylic acid plasma polymerisation. This scaffold was used as a structural mimic of the trabecular bone and *in vitro* determination of biocompatibility using cultured bone cells (MG63) demonstrated that cells were able to colonise all materials tested, with evidence that acrylic acid plasma polymerisation improved biocompatibility in the long term. The osteosarcoma cell culture on the 3D printed scaffold exhibits different growth behaviour than observed on tissue culture plastic or a flat disk of the porous material; tumour spheroids are observed on parts of the scaffolds. The growth of these spheroids indicates that the osteosarcoma behave more akin to *in vivo* in this 3D mimic of trabecular bone. It was concluded that PolyHIPEs represent versatile biomaterial systems with considerable potential for the manufacture of complex devices or scaffolds for regenerative medicine. In particular, the possibility to readily mimic the hierarchical structure of native tissue enables opportunities to build *in vitro* models closely resembling tumour tissue.

Keywords: High Internal Phase Emulsion, PolyHIPEs, scaffold, emulsion templating, photopolymerisation, bone cells, MG63

*Corresponding author for biocompatibility determination: Paul V. Hatton, Bioengineering and Health Technologies Group, The School of Clinical Dentistry, University of Sheffield, Sheffield S10 2TA, United Kingdom; Email: paul.hatton@sheffield.ac.uk

**Corresponding author for microfabrication: Frederik Claeyssens, Biomaterials and Tissue Engineering Group, Department of Materials Science and Engineering, Kroto Research Institute, University of Sheffield, Sheffield S3 7HQ, United Kingdom, Email: F.Claeyssens@shef.ac.uk

Received: April 8, 2016; **Accepted:** June 1, 2016; **Published Online:** June 24, 2016

Citation: Malayeri A, Sherborne C, Paterson T, *et al.*, 2016, Osteosarcoma growth on trabecular bone mimicking structures manufactured via laser direct write. *International Journal of Bioprinting*, vol.2(2): 67–77. <http://dx.doi.org/10.18063/IJB.2016.02.005>.

Introduction

PolyHIPEs are a class of materials where porosity is introduced using a phase separated mixture by a process often termed as emulsion templating, in which the continuous phase of high internal phase emulsions (HIPE) is polymerised. The PolyHIPE structure shows promise for 3D cell culture, as the porosity may be tailored to produce different structures that have the potential to modify *in vitro* cell response^[1]. For example, the production of larger voids can be achieved through controlled coalescence of the HIPE before polymerisation by rupturing of the barrier film^[2] by increasing the original emulsion temperature or through the addition of organic additives^[1]. Typically surface area ranging between 3–20 m²·g⁻¹ may be achieved and increased further by replacing a proportion of the continuous monomer phase with non-polymerisable solvents^[2,3].

Generally, PolyHIPEs are created via thermal polymerisation of the continuous phase which can take up to 24 hours^[4]. The most widely used monomers in PolyHIPE chemistry are styrene and its derivatives, and often the crosslinker divinylbenzene, due to their hydrophobic properties^[1,2,5,6]. Nevertheless, there are reports of PolyHIPE preparations with acrylate-based monomers such as 2-ethylhexyl acrylate (EHA), isobornyl acrylate (IBOA) and butyl acrylate (BA)^[1,5,6]. The addition of EHA increases the elasticity of the polymer matrix and its hydrophobic properties lowers the interfacial tension between the two phases which results in a lower void diameter^[7]. Producing PolyHIPE blends of EHA^[4,8], typically with IBOA, provides a route to control the mechanical properties. These materials are water immiscible and offer adequate rigidity to support cell proliferation which can be improved by the inclusion of acrylic acid^[9]. However, they have a non-degradable aliphatic carbon backbone that limits their applications to *in vitro* use. Photopolymerisation of acrylates to create PolyHIPEs was first reported in 2006^[10] via photo-initiators^[11]. A study by Pierre *et al.* employed EHA and IBOA monomers with trimethylolpropane triacrylate (TMPTA) crosslinker and Span 80 as surfactant, showing the effect of the monomer choice (EHA or IBOA) on the elastic properties of the monolith as well as employing photoinitiated polymerisation as a curing method^[10]. Photoinitiated polymerisation reduces the cure time to seconds, which means that less stable emulsions can be cured which might otherwise destabilise during the

long process of thermal curing or with increase in temperature^[2,4,10,12]. This approach has potentially increased the versatility of PolyHIPE systems, and there is a growing interest in the use of photocurable monomers for their production^[4,8,11–16]. PolyHIPEs have been commercialised for use as 3D environments for cell culture including the development of more complex tissue models. In these applications it was reported that the 3D structure encourages the formation of a more physiologically correct tissue structure, and the microporosity may facilitate mass transfer when used in combination with a bioreactor^[17]. Despite the benefits of a 3D PolyHIPE scaffold, only simple shapes are available and mass transfer is relatively limited. For example, the internal pore size in commercial systems such as Alvetex (Reinervate Ltd.) generally has a narrow pore size distribution of 36 to 40 μm^[1].

Since the emergence of additive manufacturing, the production of scaffolds with more complex shapes, e.g., in a specific bioreactor or to engineer an advanced tissue construct, has been a rich research field, and currently different technologies have been reported for production of biomaterial scaffolds with complex or custom shapes and hierarchical porosity. For example, additive manufacturing can be used in combination with electrospinning to produce 3D porous structures for tissue engineering^[18,19]. Additionally, indirect additive manufacturing, where a 3D structure of a sacrificial material is printed and subsequently a porogen-containing material is cast in the voids. The material is washed to remove both the sacrificial scaffold and the porogen. This method has been demonstrated to produce both vili-shaped surface relief patterns and 3D woodpile-structured with internal porosity^[20,21]. The use of a sacrificial scaffold has also been used in conjunction with electrospinning to produce microporous electrospun mats with internal channels to introduce a prototype vascular network in these scaffolds^[22,23].

Recent studies reported on the use of layer-by-layer stereolithography for selectively photocuring PolyHIPE emulsions to fabricate customised structures with both random microporosity and controlled macroporosity^[11,13,24]. In this process, the templated emulsion is used as the resin for the direct write process. The advantage of this process (i) to the indirect additive manufacturing process is that the scaffold is written directly in the porous material, with no need of building sacrificial materials, and (ii) to additive

electrospinning is that the speed of making the scaffolds is much higher when using HIPEs. The scaffolds reported in this study are produced in minutes, while electrospinning would typically take hours to build similar thickness scaffolds. An additional advantage of using HIPEs for 3D structuring is the easy inclusion of nanoparticles in the formulations by using Pickering HIPEs. Recently, we demonstrated that hydroxyapatite particles can be incorporated in these resins and can be used for 3D structuring^[25].

The hierarchical porosity of these scaffolds plays a crucial role as smaller pores limit the migration of cells into the scaffold while improving mass transfer, therefore constraining the cell growth to the outer surface^[26]. Synthetic materials have been used for this purpose as they can provide reproducibility in regards to purity and tuneability of the material properties to control the tissues' response^[16]. Highly macro- and microporous polymers are appealing candidates for tissue engineering applications due to their inherent 3D porous interconnected nature, structural strength and tunable mechanical properties^[27]. The aim of this research was to investigate the development of biocompatible non-degradable PolyHIPE materials that could present two levels of structural hierarchy, microporosity to achieve optimal cell ingrowth and macroporosity to mimic larger tissue structural ordering. In this study we focus on building a structural mimic of trabecular bone and we have studied the growth of osteosarcoma on these structures.

2. Experimental Methods

2.1 Materials

Monomers [isobornyl acrylate (IBOA) and 2-ethylhexyl acrylate (EHA)], crosslinker (trimethylolpropane triacrylate) and the photoinitiator diphenyl(2,4,6-trimethylbenzoyl) phosphine oxide/2-hydroxy-2-methylpropiophenone were all purchased from Sigma-Aldrich (UK). Hypermer B246 (Croda, UK) was used as a surfactant. All materials were used without further purification or modification. Cell culture media was obtained from Invitrogen (Paisley, UK) and supplements from Sigma-Aldrich (UK).

2.2 PolyHIPE Sample Preparation

Hypermer B246 surfactant (0.2 g) and the organic compounds EHA (3.7 g), IBOA (1.6 g) and triacrylate (1.4 g) were mixed together until the surfactant had dissolved. The photoinitiator was added (5 wt % of the organic

compounds EHA, IBOA and triacrylate). The components were mixed using a paddle stirrer (Pro40 Sci-Quip) at 350 rpm while water was added drop by drop; the mixture was then left to mix for 5 minutes. The HIPE was transferred to a glass vial for either the direct laser write or bulk polymerisation. Bulk photopolymerisation of the PolyHIPE was carried out using a UV belt curer (GEW Mini Laboratory, GEW engineering UV) with a 100 W·cm⁻² UV bulb. The sample was passed several times under the UV lamp at a speed of 5 m·min⁻¹ on both sides. The resulting monoliths were immersed in acetone (100 mL for 24 hours). Samples were dried in a vacuum oven and dried under vacuum afterwards until reaching constant mass.

Woodpile structures were manufactured from EH-A80 using single photon direct laser write. A passively Q-switched DPSS microchip laser (PULSELAS-P355-300, ALPHALAS) emitting both 532 and 355 nm was used as the light source. The 355 nm UV light was separated using a Pellin-Broca prism (ADB-10, THORLABS), and expanded using a Galilean beam expander to approximately 8 mm diameter. The on/off stage of the light is controlled using the shutter (UNIBLITZ LS6, Vincent Associates) linked to a shutter driver (VCM-D1, Vincent Associates). An adjustable pinhole was used to produce a uniform circular beam of UV light prior to entering the microscope objective (EC-Plan NEOFLUAR 10x, ZEISS), which focused the beam onto the sample holder affixed to a high precision xyz stage, (ANT130-XY, Aerotech for *xy* translation & PRO115, Aerotech for *z* translation), the motion was controlled using the motion control software A3200 (Aerotech). This stage was used to translate the HIPE-based resin relative to the objectives' focal spot. HIPE (120 µL) was pipetted into a functionalised 13 mm glass coverslip placed inside a temporary silicone well affixed on top of a glass slide. The laser was passed over the top surface to polymerise the woodpile lines; 50 µL of HIPE was pipetted on top of the previously cured layer PolyHIPE and the process was repeated 3 times to produce the woodpile structures. The samples were washed in acetone for 24 hours, and then vacuum dried until reaching a constant weight. The samples were sterilised in 70% ethanol for 45 minutes and washed 3 times with phosphate buffered saline (PBS) prior to any cell culture.

Plasma coating was performed in an in-house system formed from a cylindrical borosilicate chamber with stainless steel endplates. Chamber pressure was detected by an active Pirani gauge (APG-L-NW25 Ed-

wards) and pressure was controlled by a needle valve (Edwards LV10K). The flow rate of acrylic acid monomer was established through the chamber at $2.4 \text{ cm}^3 \text{ min}^{-1}$. The electromagnetic field was generated by radiofrequency generator (Coaxial power systems limited) through a coil wrapped around the chamber. The power to this coil was set to 15 W and the plasma was left on for 20 minutes.

2.3 *In Vitro* Biocompatibility

In vitro biocompatibility of PolyHIPE materials in the form of both EHA80 disks and woodpile structures was investigated using the human osteosarcoma cell line MG-63. MG-63s were cultivated in Dulbecco's modified Eagle's medium (DMEM) supplemented with 10% fetal calf serum, 1% penicillin and streptomycin, 1% L-glutamine and 0.25% amphotericin B in a humidified 5% CO_2 atmosphere at 37°C . Cells were seeded on PolyHIPE disks and woodpile scaffold structures and incubated for 7 days *in vitro*. PolyHIPE scaffolds and disks were placed in 12-well plates and secured using marine grade steel rings (2 cm outer diameter, 1 cm inner diameter). The disks were seeded at a density of 20,000 cells per disk ($n = 6$ of each type per day) and the woodpile scaffolds were seeded at a density of 100,000 cells per scaffold. The required numbers of cells were seeded on the samples in $10 \mu\text{L}$ of DMEM cell suspension placed in the centre of the samples and was left in an incubator for 50 minutes at 37°C . A further $990 \mu\text{L}$ of DMEM was added to each well and were left in the incubator for the duration of the experiment (1, 3 and 7 days). Media was changed every two days. The controls ($n = 6$) involved seeding cells on tissue culture plastics containing the standard medium. All the disks were incubated at 37°C in 5% CO_2 for 1, 3 and 7 days.

MTT assay is a quantitative indicator of metabolically active cells, which is widely used as an indicator to analyse cell proliferation as well as cell viability. The MTT [3-(4,5)-dimethylthiazol-2-yl]-2,5-diphenyl-tetrazolium bromide] solution was prepared in advance at a concentration of $0.5 \text{ mg}\cdot\text{mL}^{-1}$. The samples were washed in PBS and 1 mL of MTT solution was added to each disk and was left in the incubator for 50 minutes. The disks were washed slowly with PBS to minimise any risks involved in the accidental removal of produced formazan salts. Ethoxyethanol reagent plus (700 μL) solvent (Sigma, UK) was added to each sample to dissolve the formazan crystals resulting from MTT reduction. The samples were left on a me-

chanical rocker for 24 hours to ensure complete dissolving of formazan crystals prior to the removal of 200 μL of MTT solution (triplicate readings) from each sample. The absorbance of the solution was measured using a Biotek absorbance reader (Model Elx800) at a single wavelength of 562 nm. Statistical analysis of the results was carried out using the Graphpad Prism program. The significance between the control and test values was compared using the two tailed *t*-test with an assumption of equal variance. The levels of significance are indicated in the graphs.

2.4 Cell Imaging: Scanning Electron Microscopy, Confocal Microscopy

The morphology of PolyHIPE structures and MG63 cells was investigated using Philips XL-20 scanning electron microscope operating at 10.0 kV. The PolyHIPE disks were washed in PBS three times and fixed in 2.5% glutaraldehyde for 1 hour. The samples were further washed in PBS, and then soaked in distilled water for a further 5 minutes. Finally, the disks were dehydrated for 15 minutes in a series of ethanol solutions at 35%, 60%, 80%, 90% and 100% concentration. The disks were finally treated with HDMS/EtOH (1:1 EtOH + HDMS) for 1 hour following a rinsing in 100% HDMS for 5 minutes. The samples were air dried prior to sputter coating with gold and prior to be attached by adhesive carbon tabs onto aluminium stubs. SEM images were taken from different sections of the same PolyHIPE structure and random selection of 25 voids from each SEM image was made and statistical correction factor was applied to the average void diameter^[1]. The average void diameter of the structures was quantified using the software ImageJ 1.48.

The cell seeded woodpile structures were used for SEM. Single plane images (1024×1024 pixels) were obtained using a Zeiss LSM Meta upright confocal microscope. Z-stack images (512×512 pixels) were obtained using the same settings as single plane images but repeated images were obtained of the same area, translated 11 μm in the z direction after each capture. After fixation with 3.7% formaldehyde (approximately 30 minutes) at room temperature, the woodpile structures were permeabilised with Triton-X100 (1%) for approximately 3 minutes. Cells were washed further with PBS three times. Finally, the cells were treated with 0.1% nuclear staining DAPI and 0.1% Phalloiding-FITC. DAPI was excited via a two-photon 800 nm laser (11% transmission) and the emission detected between 435 and 485 nm. FITC-

Phalloidin was excited using a 488 nm laser (4% transmission) and emission detected above 505 nm. For differential interference contrast (DIC), a 543 nm laser (21.8% transmission) was used without filters to produce a contrast of scaffold. Z-stacks were converted to single images using ImageJ's Z-project feature using the max intensity blend setting. Images were measured and scale bars were also added by ImageJ.

3. Results and Discussion

3.1 Morphological Characterisation

The morphology and surface structure of the woodpile structures were analysed using SEM. Typical PolyHIPE morphology was maintained within the scaffolds, suggesting the selective polymerisation of the PolyHIPE did not adversely affect the internal porosity. The creation of a surface skin has been reported in literature when the HIPE collapses at the surface, for

example a closed surface is observed when the HIPE is cured against polypropylene^[2]. Similar features were observed in the HIPE emulsion when selectively curing regions within the bulk emulsion. The boundary between the cured and uncured HIPE formed a surface skin during the post-processing stages to wash and dry the PolyHIPE structures. This is attributed to a structural collapse of a partially cured boundary layer on the surface of the PolyHIPE. There are two plausible explanations for this phenomenon: (i) the HIPE material acted as a scattering medium for the curing UV light, and (ii) the diffusion of reactive radicals from the photo-initiated region.

The microporosity can be controlled by the speed of the paddle stirrer. The pore size of the polyHIPE produced at a stir speed of 350 rpm was determined using SEM (Figure 1). ImageJ was used to measure the pore diameters from fractured PolyHIPE structures and to account for the underestimation of the measured

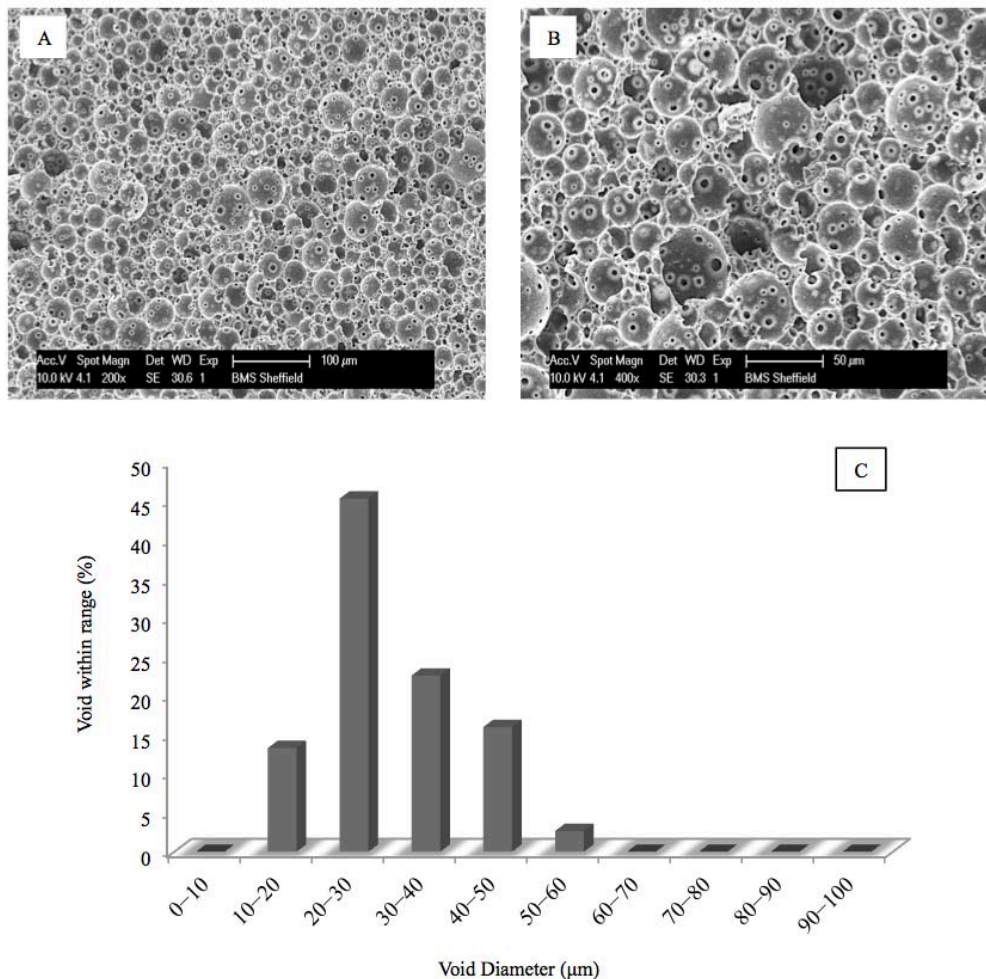


Figure 1. PolyHIPE disk morphology. (A) Morphology of 80% EHA80 PolyHIPE disks obtained by SEM – Scale bar 100 µm, (B) Scale bar 50 µm. (C) Void diameter distribution of PolyHIPE disks based on SEM micrograph analysis.

pores, a statistical correction factor was used to create a more accurate estimate of the actual pore diameter^[3]. The average pore diameter for EHA80 PolyHIPE is 33.3 μm (mean standard deviation $\pm 10.6 \mu\text{m}$).

The woodpile structures presented similar behaviour. Increasing the IBOA content increases the stiffness of the material and reduces the swelling. For scaffolds with high EHA content, the PolyHIPE can be freeze dried to prevent the PolyHIPE from shrinking as it dries^[10].

Woodpile layered structures from a high internal phase emulsion are fabricated successively to create selectively cured regions of PolyHIPE in a stereolithography-based direct laser writing approach. This was achieved by selectively curing the top layer of a well of the HIPE emulsion, and subsequently adding layers of the emulsion and curing them to build up an object in a layer-by-layer manner (Figure 2). This leads the way for more complex structures to be made. However, increasing the size or number of layers will increase the build time per scaffold. The total build time per scaffold was less than 10 minutes and the scaffold parameters were nearly identical by visual inspection. The final structures were demonstrated to be suitable for 3D cell culture applications and mimic

the macroporosity of the trabecular bone. The trabecular bone exhibits a macroporosity of 300–600 μm and a porosity of 75–85%^[28]. The produced scaffolds have a strut size of 250 μm and a fibre spacing of 1100 μm , while exhibiting a macroporosity of 82% and a pore size of 425 μm (given that the layers are offset by 550 μm). These scaffolds have a much higher macroscopic porosity and a larger macroscopic pore size compared to the structures reported in our previous study (58% macroporosity and 150 μm pores)^[24]. Young's modulus of the 80% porous material is 1.22 MPa^[24].

3.2 Osteosarcoma Growth

In this study, we assessed the growth of human osteosarcoma (MG-63) on these 3D printed scaffolds. Our PolyHIPE structure is based on a mixture of the elastomer component EHA and the brittle component IBOA (at a 66–33% w/w ratio). These PolyHIPEs are typically produced as monoliths with the pore size solely determined by the emulsion templating process. These pore sizes are typically of the order of 10–50 μm , which can impede cell ingrowth and materials transfer. To mitigate for this, previous studies used a high water volume of 90% and an elevated temperature to destabilise the emulsion for larger pore sizes^[1]. In our

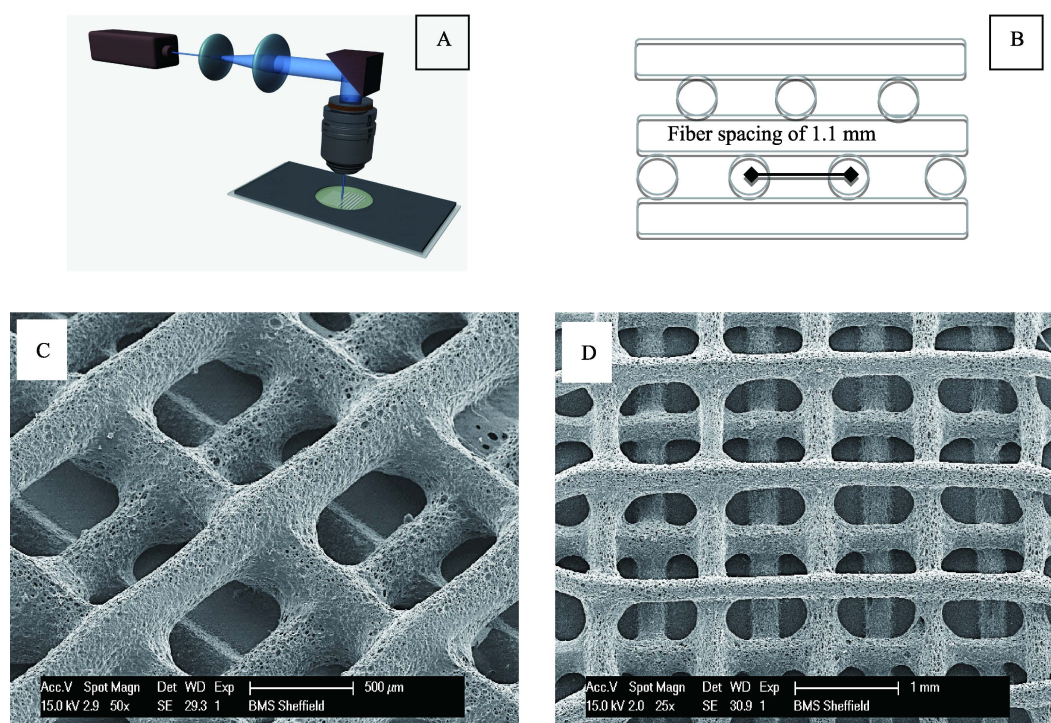


Figure 2. (A) Woodpile structure fabricated via single photon direct laser write with dimensions of $0.5 \times 0.5 \text{ cm}$, (B) Schematic representation of the woodpile structure with fibre spacing of 1.1 mm and total dimensions of $0.5 \times 0.5 \text{ cm}$. (C–D) Morphology of the 80% nominal porosity EHA PolyHIPE woodpile structure obtained by SEM (scale bar = 500 μm), (D) Scale bar = 1 mm.

approach, the inherent porosity dictated by the emulsion templating is retained, while the larger pore sizes (to enhance materials transport and ingrowth) are built by laser-based direct write.

For tissue engineering scaffolds, it is important to consider additional features beyond structural architecture, including surface chemistry which affects cellular attachment^[15]. With regards to this, the inherent hydrophobic nature of the PolyHIPE material needs to be addressed. This is an inevitable consequence of the required hydrophobicity of the original monomers to create the HIPE emulsion. Therefore, we used plasma treatment to post-modify the surface of the PolyHIPE structures prior to cell culture. Plasma treatment increased the hydrophilicity, and thus the initial cell attachment of the PolyHIPE surface without affecting the bulk PolyHIPE morphology^[22].

In vitro cell culture studies were undertaken to assess the potential use of these scaffolds as 3D bone

tissue engineering constructs. A human osteosarcoma cell line (MG63) was cultured on bulk and woodpile PolyHIPE for up to 7 days as well as tissue culture plastic as positive control. Figure 3 and Figure 4 show successful culture of MG63 cells on both EHA80 PolyHIPE disks and woodpile structures. Cell viability was evaluated via MTT assay on day 1, 3 and 7. Cell viability of acrylic acid coated PolyHIPE disks was higher than control in all time points. However, as shown in Figure 4A both acrylic acid coated and non-coated woodpile structures showed lower cell activity compared to the control, but the biocompatibility of the materials was demonstrated. Cells grown on the scaffolds had a larger surface area to the 2D counterpart; therefore we have normalised the assays to account for this. A separate study was carried out to determine what percentages of cells were seeded successfully on the woodpile structure in comparison to the control. The investigation showed that only 36%

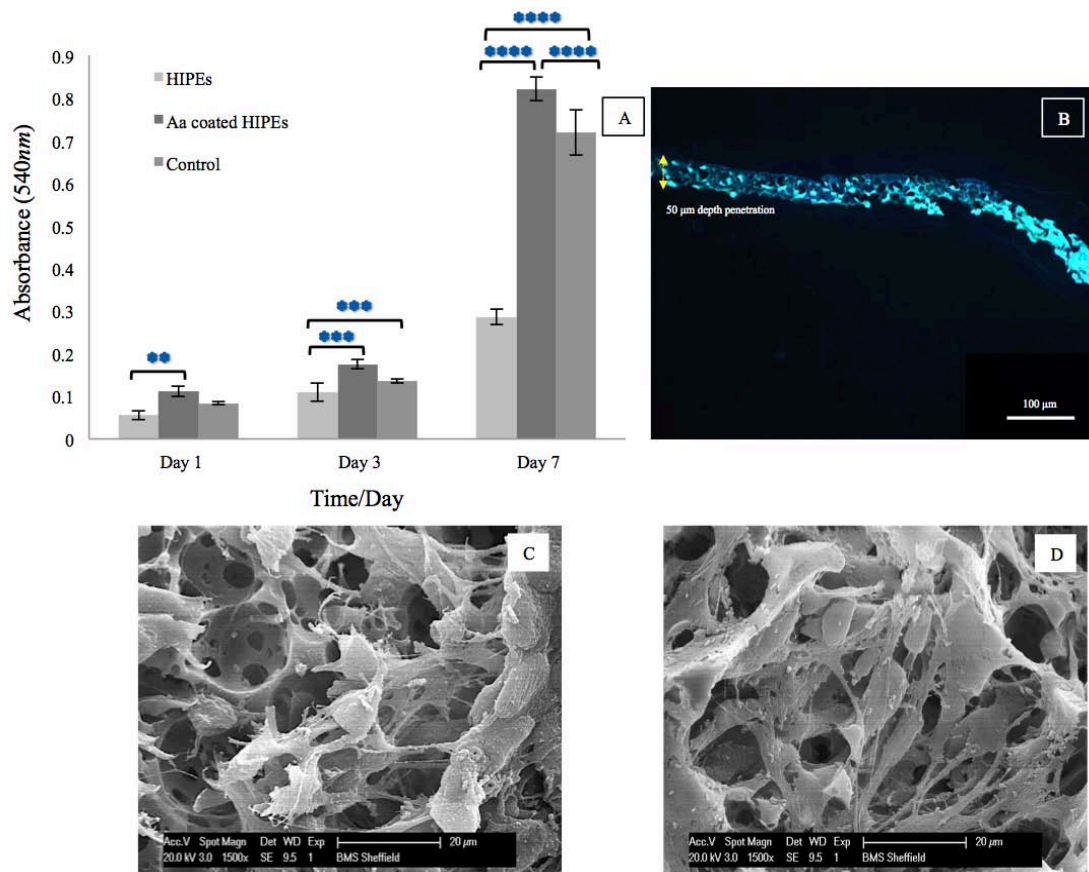


Figure 3. *In vitro* experiment with PolyHIPE disks. (A) MTT assay for proliferation of MG63 on acrylic acid coated and non-coated PolyHIPE disks during different incubation period. Error bars represent the standard deviation of mean. (B) Immunofluorescence micrograph of cryo-sectioned PolyHIPE disk cultured with MG63 stained with DAPI and Phalloidin-FITC at day 7 – Scale bar 100 µm. (C) SEM micrographs showing the attachment of MG63 cells on non-coated PolyHIPE disks on day 7, (D) on acrylic acid coated PolyHIPE disks on day 7.

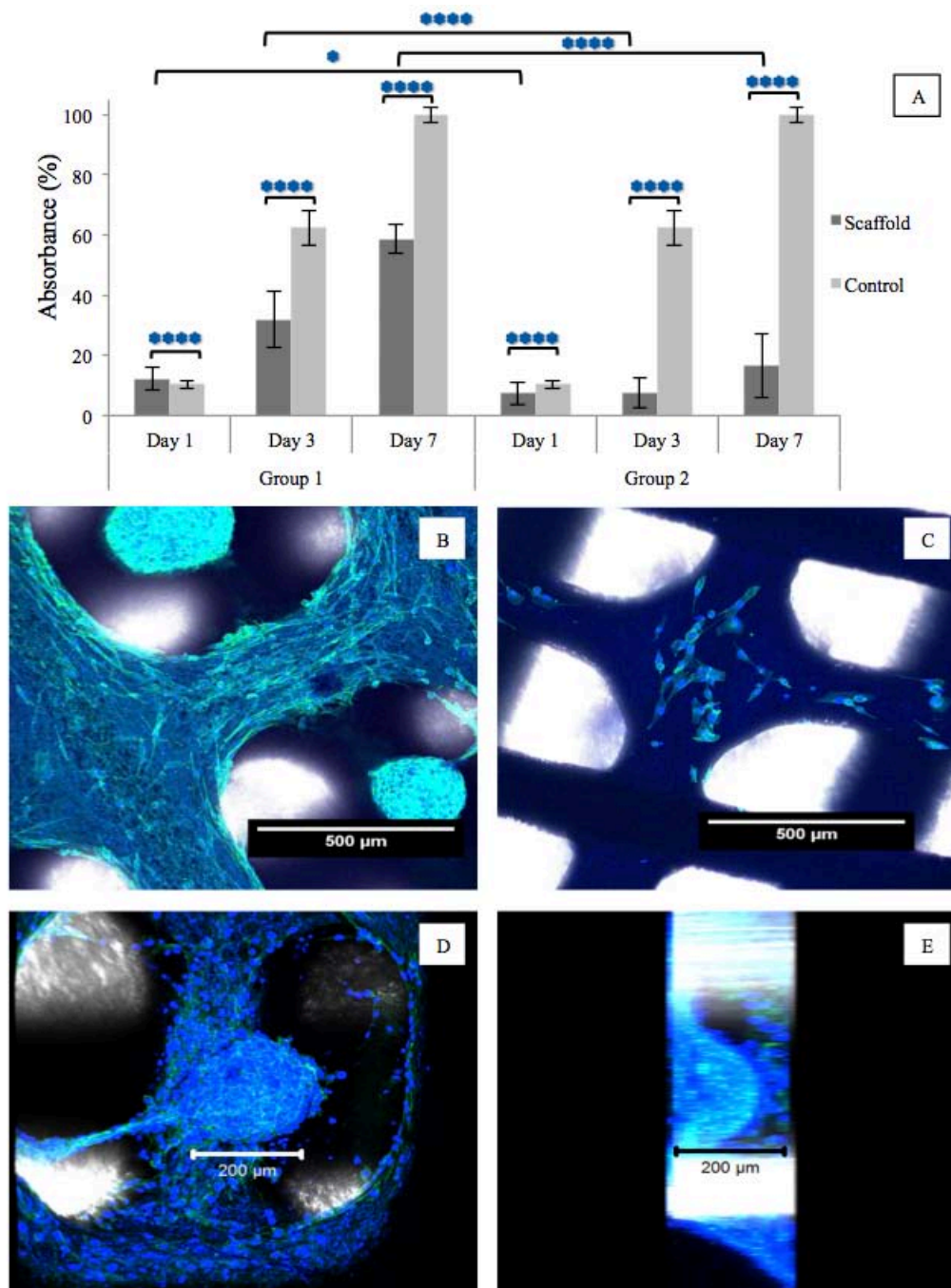


Figure 4. *In vitro* biocompatibility experiment of EHA80 woodpile scaffolds cultured with MG63 determined by MTT. (A) Viability of MG63 cell cultures on acrylic-acid coated woodpile scaffold (Group 1) and non-coated woodpile scaffolds (Group 2) shown as a plot of absorbance against time (error bars represent 95% confidence level). (B) Micrographs of acrylic-acid coated PolyHIPE woodpile scaffolds stained with DAPI and Phalloidin-FITC at day 7. (C) Non-coated woodpile structure cultured with MG63 at day 7. (D) MG63 cell spheroids formed within woodpile pores. (E) Cross sectional view of the cell spheroid.

of cell density was seeded successfully on the acrylic acid coated woodpile structure and 26% for non-coated woodpile structures in comparison to the tissue culture plastic control during the initial day 0 of cell seeding. Cell growth and penetration are shown in

SEM micrographs (Figure 3C–D) where the morphology of the cells on acrylic acid-coated PolyHIPE disks are more flat compared to the rounded cell attached to the non-coated PolyHIPE disks. As shown in Figure 3B, immunofluorescence micrographs of the

cryosectioned PolyHIPE disk demonstrate the integration and penetration of MG63 cells within the microporosity nature of PolyHIPE materials (50 μm depth). These results can be compared to our previous results of human Embryonic Stem Cell derived Progenitors (hESMPs) on similar scaffolds which highlighted that only plasma treated scaffolds supported hESMP cell growth^[24]. Additionally, the scaffolds supported differentiation towards osteoblasts in a 14-day timescale, and this was dependent on the stiffness of the scaffold.

Evidence of cell ingrowth can be observed on the immunofluorescence images of the woodpile structures; the cells are very well attached and they penetrate within the scaffold (Figure 4B). Interestingly, as shown in Figure 4D–E, spherical clusters of MG63 cells were formed within the macropores of the woodpile structures (each spheroid reaching a diameter of approximately 200 μm after 7 days). This growth behavior has not been observed on either tissue culture plastic or the PolyHIPE disk and closely resembles tumour-like spheroids. This observation indicates that the HIPE-based macroporous 3D environment encourages the osteosarcoma cell line to behave in a more natural way, forming tumour-like spheroids without the requirement of any external manipulation. Previous studies have also shown similar findings where MG63 spheroids have been developed (i) in *ex vivo* bone formation models and (ii) in *in vitro* 3D culture systems, for example, using silicate-based hydrogels^[29–31]; but the observation of culturing tumour-spheroids in a 3D *in vitro* structured scaffold has to our knowledge not yet been reported. Overall, the development of PolyHIPE-based 3D scaffolds offers more realistic opportunities for replicating *in vivo* behavior of cell environments. Therefore, this 3D PolyHIPE scaffold has potential as an *in vitro* tissue engineering model for tumour-on-chip devices.

4. Conclusion

An acrylate based PolyHIPE was prepared with a micrometer porosity of approximately 80%. The basic material was structured in a three dimensional woodpile structure using single photon direct laser writing to introduce macroporosity while retaining the inherent microporosity of the PolyHIPE and with a macrostructure that mimics the structure of cortical bone (80% porosity and 450 μm pores). Scanning electron microscopy demonstrated that PolyHIPE woodpile structures fabricated via laser-based solid freeform fabrication technology retained both of these macro- and

micro-scale porosities. This demonstrates control of porosity at different structural levels. Osteosarcoma cells (MG63) were grown on both the woodpile structure and porous disks of the materials. Cell ingrowth (50 μm in 7 days) was observed in the PolyHIPE disks, while the woodpile structures supported the growth of tumour spheroids, a growth mode that was not observed on the disks or on tissue culture plastic. The excellent biocompatibility of the parent material was not adversely affected by processing to form a complex 3D shape. In addition to preparing *in vitro* models, this technology when combined with biodegradable materials, shows significant potential for the manufacture of functional scaffolds or devices for the repair of complex tissue defects, as the direct laser writing may be applied to the fabrication of custom-shaped porous structures.

Conflict of Interest and Funding

No conflict of interest was reported by the authors.

Acknowledgments

This work was supported by the UK Engineering and Physical Sciences Research Council with a PhD studentship (EP/L014823/1) and by MeDe Innovation (the EPSRC Centre for Innovative Manufacturing in Medical Devices, grant number EP/K029592/1). Imaging work was performed at the Kroto Research Institute Confocal Imaging Facility, using the LSM510 Meta upright confocal microscope.

References

1. Bokhari M, Carnachan R J, Przyborski S A, *et al.*, 2007, Emulsion-templated porous polymers as scaffolds for three dimensional cell culture: effect of synthesis parameters on scaffold formation and homogeneity. *Journal of Materials Chemistry*, vol.17(38): 4088–4094. <http://dx.doi.org/10.1039/B707499A>
2. Kimmins S D and Cameron N R, 2011, Functional porous polymers by emulsion templating: recent advances. *Advanced Functional Materials*, vol.21(2): 211–225. <http://dx.doi.org/10.1002/adfm.201001330>
3. Barbetta A and Cameron N R, 2004, Morphology and surface area of emulsion-derived (PolyHIPE) solid foams prepared with oil-phase soluble porogenic solvents: span 80 as surfactant. *Macromolecules*, vol.37(9): 3188–3201. <http://dx.doi.org/10.1021/ma0359436>
4. Kimmins S D, Wyman P and Cameron N R, 2012, Photopolymerised methacrylate-based emulsion-templated porous polymers. *Reactive and Functional Polymers*,

- vol.72(12): 947–954.
<http://dx.doi.org/10.1016/j.reactfunctpolym.2012.06.015>
5. Foudazi R, Gokun P, Feke D L, *et al.*, 2013, Chemorheology of Poly(high internal phase emulsions). *Macromolecules*, vol.46(13): 5393–5396.
<http://dx.doi.org/10.1021/ma401157b>
 6. Gitli T and Silverstein M S, 2008, Bicontinuous hydrogel-hydrophobic polymer systems through emulsion templated simultaneous polymerizations. *Soft Matter*, vol.4(12): 2475–2485.
<http://dx.doi.org/10.1039/B809346F>
 7. Moghbeli M R and Shahabi M, 2011, Morphology and mechanical properties of an elastomeric poly(HIPE) nanocomposite foam prepared via an emulsion template. *Iranian Polymer Journal*, vol.20(5): 343–355.
 8. Cummins D, Wyman P, Duxbury C J, *et al.*, 2007, Synthesis of functional photopolymerized macroporous polyHIPEs by atom transfer radical polymerization surface grafting. *Chemistry of Materials*, vol.19(22): 5285–5292.
<http://dx.doi.org/10.1021/cm071511o>
 9. Hayward A S, Sano N, Przyborski S A, *et al.* 2013, Acrylic-acid-functionalized PolyHIPE scaffolds for use in 3D cell culture. *Macromolecular Rapid Communications*, vol.34(23–24): 1844–1849.
<http://dx.doi.org/10.1002/marc.201300709>
 10. Pierre S J, Thies J C, Dureault A, *et al.*, 2006, Covalent enzyme immobilization onto photopolymerized highly porous monoliths. *Advanced Materials*, vol.18(14): 1822–1826.
<http://dx.doi.org/10.1002/adma.200600293>
 11. Sušec M, Ligon S C, Stampfl J, *et al.*, 2013, Hierarchically porous materials from layer-by-layer photopolymerization of high internal phase emulsions. *Macromolecular Rapid Communications*, vol.34(11): 938–943.
<http://dx.doi.org/10.1002/marc.201300016>
 12. Caldwell S, Johnson D W, Didsbury M P, *et al.*, 2012, Degradable emulsion-templated scaffolds for tissue engineering from thiol-ene photopolymerisation. *Soft Matter*, vol. 8(40): 10344–10351.
<http://dx.doi.org/10.1039/C2SM26250A>
 13. Johnson D W, Sherborne C, Didsbury M P, *et al.*, 2013, Macrostructuring of emulsion-templated porous polymers by 3D laser patterning. *Advanced Materials*, vol.25(23): 3178–3181.
<http://dx.doi.org/10.1002/adma.201300552>
 14. Lovelady E, Kimmins S D, Wu J, *et al.*, 2011, Preparation of emulsion-templated porous polymers using thiol-ene and thiol-yne chemistry. *Polymer Chemistry*, vol.2(3): 559–562.
<http://dx.doi.org/10.1039/C0PY00374C>
 15. Huš S and Krajnc P, 2014, PolyHIPEs from methyl methacrylate: hierarchically structured microcellular polymers with exceptional mechanical properties. *Polymer*, vol.55(17): 4420–4424.
<http://dx.doi.org/10.1016/j.polymer.2014.07.007>
 16. Causa F, Netti P A and Ambrosio L, 2007, A multifunctional scaffold for tissue regeneration: the need to engineer a tissue analogue. *Biomaterials*, vol.28(34): 5093–5099.
<http://dx.doi.org/10.1016/j.biomaterials.2007.07.030>
 17. Griffith L G and Swartz M A, 2006, Capturing complex 3D tissue physiology *in vitro*. *Nature Reviews Molecular Cell Biology*, vol.7: 211–224.
<http://dx.doi.org/10.1038/nrm1858>
 18. Dalton P D, Vaquette C, Farrugia B L, *et al.*, 2013, Electrospinning and additive manufacturing: converging technologies. *Biomaterials Science*, vol.1: 171–185.
<http://dx.doi.org/10.1039/C2BM00039C>
 19. Ortega I, Ryan A J, Deshpande P, *et al.*, 2013, Combined microfabrication and electrospinning to produce 3-D architectures for corneal repair. *Acta Biomaterialia*, vol.9(3): 5511–5520.
<http://dx.doi.org/10.1016/j.actbio.2012.10.039>
 20. Lee M, Dunn J C Y and Wu B M, 2005, Scaffold fabrication by indirect three-dimensional printing. *Biomaterials*, vol.26(20): 4281–4289.
<http://dx.doi.org/10.1016/j.biomaterials.2004.10.040>
 21. Mohanty S, Sanger K, Heiskanen A, *et al.*, 2016, Fabrication of scalable tissue engineering scaffolds with dual-pore microarchitecture by combining 3D printing and particle leaching. *Materials Science and Engineering: C*, vol.61: 180–189.
<http://dx.doi.org/10.1016/j.msec.2015.12.032>
 22. Ortega I, Dew L, Kelly A G, *et al.*, 2015, Fabrication of biodegradable synthetic perfusable vascular networks via a combination of electrospinning and robocasting. *Biomaterials Science*, vol.3(4): 592–596.
<http://dx.doi.org/10.1039/C4BM00418C>
 23. Jeffries E M, Nakamura S, Lee K W, *et al.*, 2014, Micropatterning electrospun scaffolds to create intrinsic vascular networks. *Macromolecular Bioscience*, vol.14(11): 1514–1520.
<http://dx.doi.org/10.1002/mabi.201400306>
 24. Owen R, Sherborne C, Paterson T, *et al.*, 2015, Emulsion templated scaffolds with tunable mechanical properties for bone tissue engineering. *Journal of Mechanical Behavior of Biomedical Materials*, vol.54: 159–172.
<http://dx.doi.org/10.1016/j.jmbbm.2015.09.019>
 25. Wang A, Paterson T, Owen R, *et al.*, 2016, Photocurable high internal phase emulsions (HIPEs) containing hydroxyapatite for additive manufacture of tissue engineering scaffolds with multi-scale porosity. *Materials Science and Engineering: C*, vol.67: 51–58.
<http://dx.doi.org/10.1016/j.msec.2016.04.087>

26. Lumelsky Y, Lalush-Michael I, Levenberg S, *et al.*, 2009, A degradable, porous, emulsion-templated polyacrylate. *Journal of Polymer Science Part A Polymer Chemistry*, vol.47(24): 7043–7053.
<http://dx.doi.org/10.1002/pola.23744>
27. Silverstein M S, 2014, Emulsion-templated porous polymers: a retrospective perspective. *Polymer*, vol.55(1): 304–320.
<http://dx.doi.org/10.1016/j.polymer.2013.08.068>
28. Chen P Y and McKittrick J, 2011, Compressive mechanical properties of demineralized and deproteinized cancellous bone. *Journal of Mechanical Behavior of Biomedical Materials*, vol.4(7): 961–973.
<http://dx.doi.org/10.1016/j.jmbbm.2011.02.006>
29. Santini M T, Rainaldi G, Romano R, *et al.*, 2004, MG-63 human osteosarcoma cells grown in monolayer and as three-dimensional tumor spheroids present a different metabolic profile: a ^1H NMR study. *FEBS Letters*, vol.557(1–3): 148–154.
[http://dx.doi.org/10.1016/S0014-5793\(03\)01466-2](http://dx.doi.org/10.1016/S0014-5793(03)01466-2)
30. Trojani C, Weiss P, Michiels J F, *et al.*, 2005, Three-dimensional culture and differentiation of human osteogenic cells in an injectable hydroxypropylmethylcellulose hydrogel. *Biomaterials*, vol.26(27): 5509–5517.
<http://dx.doi.org/10.1016/j.biomaterials.2005.02.001>
31. Kale S, Biermann S, Edwards C, *et al.*, 2000, Three-dimensional cellular development is essential for *ex vivo* formation of human bone. *Nature Biotechnology*, vol.18: 954–958.
<http://dx.doi.org/10.1038/79439>